
Proceedings Paper:
Mortimer, L.F. and Fairweather, M. (2024) Role of Shear Rate on Adsorption Conformation in Polymer-Induced Flocculation Simulations. In: American Institute of Physics Conference Proceedings. International Conference on Applied Physics, Simulation and Computing (APSAC 2024), 20-22 Jun 2024, Rome, Italy. American Institute of Physics

---

Role of Shear Rate on Adsorption Conformation in Polymer-induced Flocculation Simulations

Lee Mortimer[1,a)] and Michael Fairweather[1, b)]

Author Affiliations
[1]*School of Chemical and Process Engineering*
University of Leeds
Woodhouse Lane, Leeds LS2 9JT
UNITED KINGDOM

Author Emails
[a)] *Corresponding author: l.f.mortimer@leeds.ac.uk*
[b)] *M Fairweather: m.fairweather@leeds.ac.uk*

Abstract. This study investigates the impact of shear rate on flocculation dynamics in particle-fluid systems through Monte Carlo analysis of ensembles of Langevin dynamic simulations. The research explores the temporal evolution of cluster properties, including mean cluster size, maximum cluster size, and radius of gyration, by varying the shear rate within the range of 0.001 to 0.010. The simulations, averaging across 70 realizations, reveal that higher shear rates promote the formation of larger clusters, indicative of enhanced particle interactions and aggregation. Interestingly, midrange shear rates, particularly at a variable shear rate $\dot{\gamma} = 0.005$, yield the largest clusters in terms of particle constituent numbers, suggesting a delicate balance between particle mobility and cluster stability. Moreover, analysis of the mean radius of gyration confirms the trend of increased cluster size with higher shear rates, highlighting the capacity of elevated shear rates to facilitate the formation of larger, but less compacted, clusters over larger distances. This research demonstrates the significance of shear rate in influencing flocculation dynamics and provides insights into the mechanisms governing polymer-particle interactions within shear flows.

Key-Words. Polymer simulation, flocculation, Langevin dynamics, shear flows, adsorption, polymer-particle interaction.

INTRODUCTION

The addition of small amounts of high molecular weight polymers to particle-fluid systems shows promise for numerous processing techniques, such as separating fine solids in liquid suspensions [1]. This method has proven effective in enhancing processes such as filtration and thickening in various industrial applications [2], [3]. Particularly relevant to this study are its applications in nuclear decommissioning, where it significantly aids in reducing turbidity and improving settling and sediment consolidation rates [4]. The use of polymeric flocculants also extends beyond industrial settings. Addressing the immobilization and removal of trace metal elements and pesticides from rivers, whether from natural or industrial origins, is increasingly critical. These organic and inorganic contaminants are transported through water systems, and polymeric colloidal-sized particles (with diameters less than 1 μm) require induced aggregation in order to instigate the settling process. In some instances, microorganisms in the river or water ecosystem release fibrillar extracellular polymeric substances, naturally facilitating flocculation [5]. Demonstration and comprehension of the underlying polymer flocculation mechanisms are crucial for industries to be able to fine-tune polymer species, dosages, and application methods in order to maximize performance.

Despite successful demonstrations in laboratory-scale setups and wastewater streams, the mechanisms driving flocculation in such systems remain inadequately understood. Designing and optimizing gravity-driven separation processes necessitates a thorough understanding of the system's flocculation and sedimentation dynamics. Specifically, it is essential to comprehend how the emergent flocculant structures and morphologies (such as their fractal dimension and porosity) affect hindered settling regimes. Identifying the most influential size of flocculated aggregates is critical for determining the interfacial settling rate.

Over the years, various polymeric-phase modeling techniques [6] have revealed intriguing behaviors in simple systems like stagnant tanks [7] and shear or turbulent flows [8]. Polymer-particle interactions have also been studied

within the polymer synthesis industry, with such interactions further influencing the properties of polymer nanocomposites such as viscosity, glass transition temperature, and electrical conductivity [9].

[10] used Monte Carlo simulations to study the adsorption of a finite-length polymer to a surface, discovering that the polymer's conformations transitioned from a three-dimensional random coil to a nearly two-dimensional elongated coil at temperatures significantly lower than the critical adsorption point. Research suggests that the structures emerging from polymer-particle interactions depend heavily on interaction strength, which affects the proportions of chains and loops. The length of the polymer chain also significantly impacts the adsorption dynamics [11].

[12] investigated the structural characteristics of a polymer within an attractive sphere, characterizing the polymer's conformation by its radius of gyration and gyration tensor. This study produced a diverse system phase diagram, showing behaviors ranging from desorbed states to partially or entirely adsorbed conformations. [13] further examined adsorption dynamics, focusing on the conformational properties of an adsorbed polymer on a nanoparticle using off-lattice Monte Carlo and Metropolis algorithms. They described the resulting configuration in terms of trains, loops, and tails [14]. At low polymer-nanoparticle interaction strengths, all confirmations were observed, whereas high interaction strengths favored trains and tails, eliminating loops.

The potential applications of polymer additives in fragile systems, such as nuclear waste flows, rely on the advancement of a comprehensive understanding and proven effectiveness. Previous simulation and experimental studies have rarely considered the fundamental processes which lead to flocculation, nor the effects of hydrodynamic forces and shear, which have been shown to greatly impact the adsorption behavior and structure growth [15], [16]. This research seeks to both demonstrate a novel potential-based flocculation model and to unravel the underlying dynamics of polymer-particle interactions and adhesion within shear flows. The research further aims to investigate the role of shear rate on bulk emergent behavior, as well as its influence on the dynamics of adhesion, bridging, and subsequent flocculation. To achieve this, the study explores the shear rate's impact on conformation properties, such as the mean radius of gyration and fractal dimension of flocculents, discussing their implications for collision cross-sections for subsequent polymer-particle collisions promoting cluster growth, leading to eventual settling of the structure. The insights gained from this study are crucial for developing techniques that modify system behavior by tuning bulk parameters to achieve desired outcomes.

PROBLEM FORMULATION

The polymeric phase is represented as a series of bead-spring components using Langevin dynamics [1], incorporating a finite extensible nonlinear elastic (FENE) potential to capture polymer chain interactions. The model assumes that the polymer chain exerts a nonlinear elastic restoring force on each bead, which increases as the separation distance approaches the maximum extensible length. Calculations account for excluded volume through steric interactions between all solid phases, as well as the Kratky-Porod bending rigidity to account for flexibility. The particle phase is modeled as computational point spheres interacting sterically with polymer beads through a modified Lennard-Jones potential. Each monomer bead possesses diameter σ, with $\boldsymbol{r}_i^* = \boldsymbol{r_i}/\sigma$ the non-dimensional Cartesian position vector of monomer i. The dimensional position vector $\boldsymbol{r}_i$ of each bead in a polymer chain evolves through obeying the following Newtonian equation of motion [2]:

$$m_b \frac{d^2\boldsymbol{r}_i}{dt^2} = -\boldsymbol{\nabla} V_i - \xi\left(\frac{d(\boldsymbol{r}_i)}{dt} - \boldsymbol{u}_{F,i}\right) + \sqrt{2k_B T\xi}\,\boldsymbol{\eta}_i(t). \tag{1}$$

Here, m_b is the mass of the bead, t is time, V_i is the total interaction potential calculated at the bead's current position, ξ is the drag coefficient, $\boldsymbol{u}_{F,i}$ is the local fluid velocity at the bead position, k_B is the Boltzmann constant, T is temperature and $\boldsymbol{\eta}_i(t)$ is a Brownian noise term satisfying both $\langle \eta_{ia}(t)\rangle = 0$ and $\langle \eta_{ia}(t)\eta_{ib}(t')\rangle = \delta_{a,b}\delta(t-t')$. Given that a constant bead diameter, σ, is used in this study, time can be nondimensionalised using the Brownian bead timescale $\tau_b = \sqrt{m_b\sigma/k_B T}$ and space can be nondimensionalised using the bead diameter, σ. By introducing the diffusion coefficient, $D = k_B T/\xi$, Eq. (1) can be transformed as follows:

$$\frac{d^2\boldsymbol{r}_i^*}{dt^{*2}} = -\boldsymbol{\nabla} V_i^* - \frac{1}{D}\left(\frac{d\boldsymbol{r}_i^*}{dt^*} - \boldsymbol{u}_{F,i}^*\right) + \sqrt{\frac{2}{D}}\,\boldsymbol{\eta}_i^*(t^*). \tag{2}$$

An example of a polymeric chain of monomers which forms the basis for the polymeric phase is presented in Figure 1.

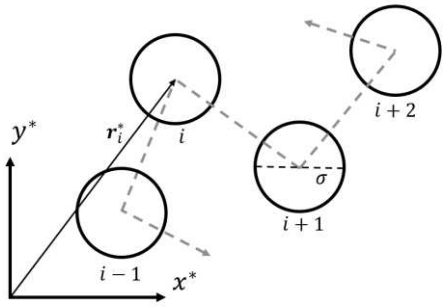

FIGURE 1. Schematic of a single modelled monomer chain forming a polymer. The dashed lines depict fictional springs connecting the monomer beads (solid circles)

The contributions to the overall non-dimensional interaction potential, V_i^*, for each bead are given by:

$$V_i^* = V_{i,F}^* + V_{i,B}^* + V_{i,W}^* + V_{i,P}^* + V_{i,WALL}^*. \tag{3}$$

Here, $V_{i,F}^*$ represents the bonds between the monomers using the FENE spring potential:

$$V_{i,F}^*(\delta r^*) = -\frac{K_F^* {R_0^*}^2}{2} ln\left[1 - \left(\frac{\delta r^*}{R_0^*}\right)^2\right], \tag{4}$$

with $\delta r^* = |\boldsymbol{r}_{i+1}^* - \boldsymbol{r}_i^*|$ the separation between two adjacent beads in the polymer chain, $K_F^* = K_F/k_B T$ the non-dimensional FENE energy scale, and R_0^* the maximum FENE bond length. This interaction potential is only considered for neighboring beads in the chain of monomers.

$V_{i,B}^*$ is the Kratky-Porod bending potential, $V_{i,B}^*(\theta_i) = K_B^*(1 + \cos(\theta_i))$, used to model the effects of bending rigidity dependant on the angle, θ_i, formed by adjacent monomer separation vectors, observed in real semi-flexible polymers. $V_{i,W}^*$ represents steric interactions between monomers and is given by the Weeks-Chandler-Anderson (WCA) potential. Polymers interact with particles through $V_{i,P}^*$, which is a truncated and shifted Lennard-Jones potential. This assumes that interactions are pairwise, isotropic, and that long-range interactions can be neglected. Finally, $V_{i,WALL}^*$ is a wall potential which is only active when the polymer position surpasses either extent of the vertical domain.

The particle equation of motion is analogous to that of the monomer beads in Eq. (2). The potential term is replaced by:

$$V_{i,P}^* = V_{i,W}^* + V_{i,P}^* + V_{i,WALL}^*, \tag{5}$$

Here, $V_{i,W}^*$ represents the interaction between particles, and $V_{i,P}^*$ denotes the interaction between particles and monomer beads. The strength of these interactions follows the same form as described in the previous subsection. Figure 2 provides an illustrative summary of the interactions between monomer beads and particles.

The simulation domain in all cases is a 100 × 100 computational channel cell in (x^*, y^*), chosen to ensure sufficient space for flocculants to form while making sure the initial injection condition concentration of both phases would lead to prompt interactions to reduce long runtimes. A Monte Carlo approach was adopted, performing $N_{MC} = 70$ full simulations within the domain to predict the mean flocculation behaviour across multiple realisations. To initialise each realisation, $N_{PAR} = 15$ particles were randomly injected throughout the domain. Depending on the number of polymers studied, an initial bead for each polymer was then injected before "growing" the polymer randomly. This was done by selecting a direction on the unit circle and injecting subsequent polymers, ensuring no overlap with previously injected beads or particles. This process continued until a total of $N_{BPP} = 32$ beads per polymer had been injected, after which the injection routine moved to the next polymer.

At each simulation step, the equations of motion for each particle and polymer bead were solved using the Verlet integration method with a constant timestep $\delta t^* = 0.002$, providing a truncation error order of $\mathcal{O}(\delta t^{*4})$. Wall conditions were enforced by activating the wall potential in both Cartesian directions beyond either extent, i.e., 0 and 100. To account for shear, the fluid velocity varied linearly with wall-distance, according to $u_F^* = \dot{\gamma} y^*$, with $\dot{\gamma}$ the variable shear rate. Each realization was performed for N_T = 40,000 timesteps ($t^* = 80$), during which time significant flocculation would occur. Simulation results are subsequently averaged across 70 independent realizations, ensuring negligible statistical error in temporal observations of cluster properties such as radius of gyration.

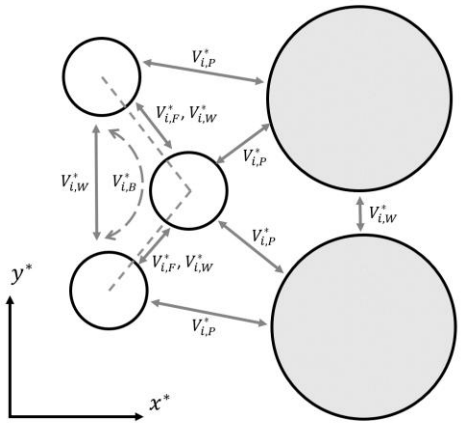

FIGURE 2. Summary of potentials involved in the interactions between two particles (gray circles) and a three-bead polymer (white circles). Gray arrows indicate the potentials included in the calculations between particle and monomers

PROBLEM SOLUTION

We consider the effect of shear on flocculation dynamics through statistical analysis of the simulations. The quantification of emergent behavior is facilitated by a Monte Carlo approach, as successfully applied in previous studies [10], [17]. Once the simulations are complete, we then average across 70 realizations to monitor and predict the temporal evolution of observables such as the mean flocculent radius of gyration and constituent numbers. The shear rate, $\dot{\gamma}$, is varied between 0.001 and 0.010. An example of a single realization is presented in Fig. 3. Over the course of the simulation, clustering occurs due to the interactions between the polymers and particles. Tails tend to be extended from the particles in the streamwise direction due to shear stretching, though a cluster of four particles can be seen to have formed near the center of the domain which is aligned perpendicular to the streamwise direction. Further investigation into temporal effects shows that this cluster was rotating due to the shear across the structure.

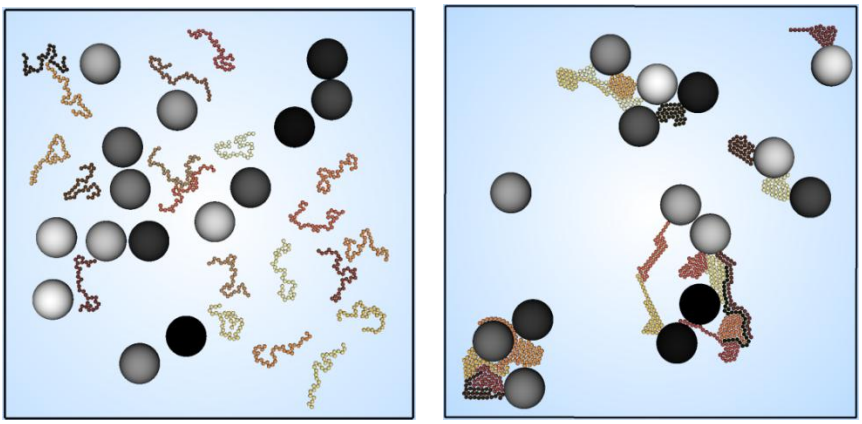

FIGURE 3. Example of one realization of Monte-Carlo simulation. Initial injection condition (left) and final flocculated state under shear flow with $\dot{\gamma} = 0.010$ (right)

Figure 4 demonstrates the effect of shear rate on the mean cluster size, C^*_{MEAN}. In all cases, by around $t^* = 60$, the simulations reach equilibrium, inferring that flocculants have reached their maximum stable size, and that breakup and adsorption events are occurring at similar rates. At the lowest shear rate, $\dot{\gamma} = 0.001$, the mean number of particle constituents in a flocculated cluster settles around $C^*_{MEAN} = 4$, meaning that there are four particles on average residing in a particular structure (two or more particles which are joined together by polymer chains). It is interesting to note that the midrange shear rate, $\dot{\gamma} = 0.005$, tends to produce the largest clusters in terms of the number of constituents. This is likely because two effects are at play: firstly, the increased shear rate enhances particle mobility and interaction, which instigates tighter bonds within the clusters; secondly, the shear rate is not so high as to disrupt the forming clusters, allowing them to grow steadily.

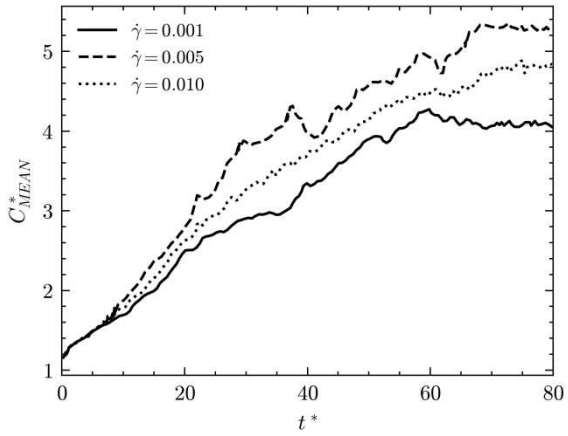

FIGURE 4. Temporal evolution of mean cluster size for flocculated clusters of particles. The effect of $\dot{\gamma}$ is demonstrated

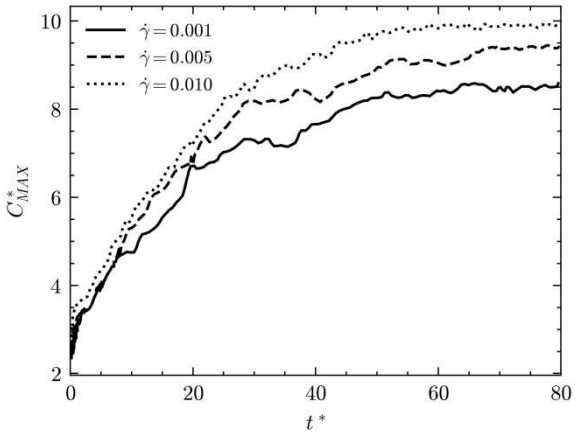

FIGURE 5. Temporal evolution of maximum cluster size for flocculated clusters of particles. The effect of $\dot{\gamma}$ is demonstrated

Figure 5 shows the effect of modifying the shear rate on the temporal evolution of the maximum cluster size, C^*_{MAX} (i.e., the maximum number of particle constituents of all clusters present in one realization). Over time, the results show divergent behavior such that systems subjected to a low shear rate, $\dot{\gamma} = 0.001$, tend to possess the smallest clusters. This is likely due to the lower energy input from the fluid phase, which limits the movement and collision frequency of particles, reducing the opportunities for cluster growth. As the shear rate increases, clusters with larger constituents can occur. At a midrange shear rate, $\dot{\gamma} = 0.005$, the increased energy facilitates more frequent collisions and interactions, leading to the formation of larger flocculants. The largest flocculants were found in the $\dot{\gamma} = 0.010$ simulation, where the higher shear rate results in more extensive movement and interaction. As the shear rate increases, the increased mobility enhances the likelihood of particle-particle and particle-polymer collisions, which are essential for initiating flocculation. Furthermore, the energy imparted by the highest shear rate facilitates more dynamic interactions, with the energy required to bind the monomer to the particle surface much more likely to be sufficient. This makes the formation of flocculants with increased constituent number energetically

possible, though since the mean cluster size is lower at $\dot{\gamma} = 0.010$, these large-constituent structures are not as stable as they are more infrequently observed.

The size of a cluster may also be characterized by its radius of gyration, which is calculated using the following expression:

$$R_G^{*2} = \frac{1}{C}\sum_{i=1}^{C}\left|\boldsymbol{r}_{P,i}^{*} - \boldsymbol{r}_{mean}^{*}\right|^2, \tag{6}$$

where C is the total number of particle constituents in a cluster, and r_{mean}^{*} is the location of the centre of area of the cluster, considering adjoining polymer chains.

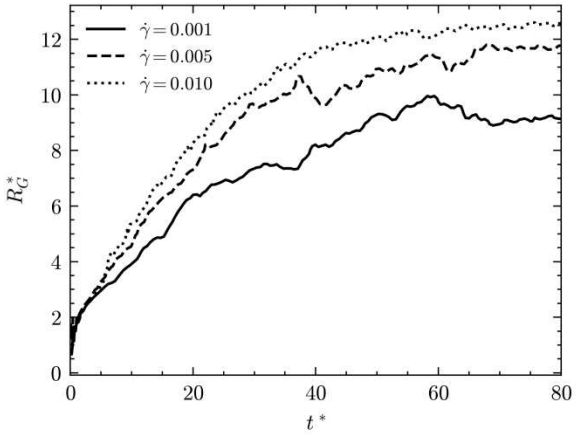

FIGURE 6. Temporal evolution of maximum cluster size for flocculated clusters of particles. The effect of $\dot{\gamma}$ is demonstrated

Figure 6 illustrates the effect of shear rate on the temporal evolution of the mean radius of gyration of clusters. In agreement with Fig. 5, the lowest shear rate, $\dot{\gamma} = 0.001$, leads to smaller clusters on average, reaching values of around $R_G^* = 9.0$, which is consistent with a tightly packed three-particle cluster. Increasing the shear rate leads to larger clusters beyond $R_G^* = 10.0$, though the adjustment from $\dot{\gamma} = 0.005$ to $\dot{\gamma} = 0.010$ shows only a small difference, despite the significant increase in mean cluster constituent numbers in Fig. 4. Even though the highest mean constituent numbers were found in the $\dot{\gamma} = 0.005$ simulation, the continued influence of the shear flow is likely to encourage particles with bridges to stretch apart, increasing the radius of gyration of the cluster. The combination of these observations implies that the increased shear rate in both cases provides the ability for similar sized flocculants to form with particle constituents possessing larger separation distances.

CONCLUSIONS

This study investigated the effect of shear rate on flocculation dynamics in particle-fluid systems using Monte Carlo analysis of Langevin dynamic simulations. By varying the shear rate across a range of values, its influence on the temporal evolution of cluster properties such as mean cluster size, maximum cluster size, and radius of gyration was examined.

The results demonstrated that higher shear rates promote the formation of larger clusters, indicating enhanced interactions and aggregation of particles. Additionally, we observed a notable dependence of mean cluster size on shear rate, with midrange shear rates producing the largest clusters. This suggests a balance between enhanced particle mobility and cluster stability under moderate shear conditions. Furthermore, analysis of the mean radius of gyration of clusters revealed a similar trend of increased cluster size with higher shear rates, indicating the ability of increased shear rate to facilitate the formation of larger clusters with particles at larger separation distances.

The results presented in this study focus on the effect of shear rate on the flocculation process and analysis of the structures formed. The use of Langevin dynamics simulations with the present potential-based formulation and non-dimensionality allows the results to stand as a useful reference for generalized behavioural modification under variation of the flow conditions. They also serve to predict the expected behavior in various regions of wall-bounded flows, where the local shear rate varies greatly with proximity to the solid boundary.

Though these simulations provide a solid groundwork for fundamental knowledge generation of these systems, to further advance our understanding of polymer-particle interactions and flocculation dynamics within shear flows, several avenues for future research should be explored. Firstly, investigating the influence of additional parameters such as polymer concentration and other contributions to the interaction potential on flocculation behavior could provide deeper insights into the underlying mechanisms. Additionally, extending the study to consider more complex systems in three dimensions with varying particle shapes and sizes should offer a more comprehensive understanding of flocculation dynamics in realistic scenarios. Finally, incorporating experimental validation of the simulation results could enhance the reliability and applicability of the findings.

ACKNOWLEDGMENTS

The authors are grateful to the UK Engineering and Physical Sciences Research Council for funding through the TRANSCEND (Transformative Science and Engineering for Nuclear Decommissioning) project (EP/S01019X/1), and Sellafield Ltd. for funding from the University of Leeds-Sellafield Ltd, Centre of Expertise for Sludge (Particulates & Fluids)

REFERENCES

1. A. R. Heath, P. A. Bahri, P. D. Fawell and J. B. Farrow, Polymer flocculation of calcite: Relating the aggregate size to the settling rate, AIChE J. **52**(6), 1987–1994 (2006). doi: 10.1002/aic.10789
2. A. P. G. Lockwood, J. Peakall, N. J. Warren, G. Randall, M. Barnes, D. Harbottle and T. N. Hunter, Structure and sedimentation characterisation of sheared $Mg(OH)_2$ suspensions flocculated with anionic polymers, Chem. Eng. Sci. **231**, 116274 (2021). doi: 10.1016/j.ces.2020.116274
3. V. Vajihinejad, S. P. Gumfekar, B. Bazoubandi, Z. R. Najafabadi and J. B. P. Soares, Water soluble polymer flocculants: Synthesis, characterization, and performance assessment, Macromol. Mater. Eng. **304**(2), 1800526 (2019). doi: 10.1002/mame.201800526
4. S. Joseph-Soly, T. Saldanha, A. Nosrati, W. Skinner and J. Addai-Mensah, Improved dewatering of clay rich mineral dispersions using recyclable superabsorbent polymers, Chem. Eng. Res. Des. **142**, 78–86 (2019). doi: 10.1016/j.cherd.2018.07.032
5. J. Buffle and G. G. Leppard, Characterization of aquatic colloids and macromolecules. 1. Structure and behavior of colloidal material, Environ. Sci. Technol. **29**(9), 2169–2175 (1995). doi: 10.1021/es00009a004
6. H. C. Öttinger, Stochastic Processes in Polymeric Fluids: Tools and Examples for Developing Simulation Algorithms (Springer-Verlag, Berlin and Heidelberg, 2012).
7. D. E. Smith, H. P. Babcock and S. Chu, Single-polymer dynamics in steady shear flow, Science **283**(5408), 1724–1727 (1999). doi: 10.1126/science.283.5408.1724
8. Z. Fu and Y. Kawaguchi, A short review on drag-reduced turbulent flow of inhomogeneous polymer solutions, Adv. Mech. Eng. **5**, 432949 (2013). doi: 10.1155/2013/432949
9. S. I. White, R. M. Mutiso, P. M. Vora, D. Jahnke, S. Hsu, J. M. Kikkawa, J. Li, J. E. Fischer and K. I. Winey, Electrical percolation behavior in silver nanowire-polystyrene composites: simulation and experiment, Adv. Funct. Mater. **20**(16), 2709–2716 (2010). doi: 10.1002/adfm.201000451
10. A. Milchev and K. Binder, Static and dynamic properties of adsorbed chains at surfaces: Monte Carlo simulation of a bead-spring model, Macromolecules **29**(1), 343–354 (1996). doi: 10.1021/ma950668b
11. H. Li, C. J. Qian and M. B. Luo, Simulation of a flexible polymer tethered to a flat adsorbing surface, J. Appl. Polym. Sci. **124**(1), 282–287 (2012). doi: 10.1002/app.34576
12. H. Arkın and W. Janke, Structural behavior of a polymer chain inside an attractive sphere, Phys. Rev. E **85**(5), 051802 (2012). doi: 10.1103/PhysRevE.85.051802
13. C. Y. Li, M. B. Luo, H. Li and W. P. Cao, Simulation study on the conformational properties of an adsorbed polymer on a nanoparticle, Colloid Polym. Sci. **295**, 2251–2260 (2017). doi: 10.1007/s00396-017-4201-y
14. C. Y. Li, W. P. Cao, M. B. Luo and H. Li, Adsorption of polymer on an attractive nano-sized particle, Colloid Polym. Sci. **294**, 1001–1009 (2016). doi: 10.1007/s00396-016-3858-y
15. A. Yeung, A. Gibbs and R. Pelton, Effect of shear on the strength of polymer-induced flocs, J. Colloid Interface Sci. **196**(1), 113–115 (1997). doi: 10.1006/jcis.1997.5140
16. R. Elhaei, R. Kharrat and M. Madani, Stability, flocculation, and rheological behavior of silica suspension-augmented polyacrylamide and the possibility to improve polymer flooding functionality, J. Mol. Liq. **322**, 114572 (2021). doi: 10.1016/j.molliq.2020.114572

17. L. F. Mortimer and M. Fairweather, Langevin dynamics prediction of the effect of shear rate on polymer-induced flocculation, Tech. Mech. **43**(1), 73–82 (2023). doi: 10.24352/UB.OVGU-2023-046